Cumhuriyet Science Journal

e-ISSN: 2587-246X
ISSN: 2587-2680

Cumhuriyet Sci. J., 42(4) (2021) 822-829
http://dx.doi.org/10.17776/csj.961752

The effects of *f*CNT and oxidation on the OGG/*f*CNT double networked hydrogel

Serbülent TÜRK [1, 2,*]

[1]*Sakarya University, Biomedical, Magnetic and Semi Conductive Materials Research Center (BIMAS-RC), Esentepe Campus, 54187 Sakarya/TURKEY*
[2]*Sakarya University, Biomaterials, Energy, Photocatalysis, Enzyme Technology, Nano & Advanced Materials, Additive Manufacturing, Environmental Applications and Sustainably Research & Development Group (BIOENAMS R&D Group), 54187, Sakarya/TURKEY*

Abstract

Double networked (DN) hydrogel systems consisting of *f*CNT and OGG have been successfully developed by ionic crosslinking. OGG was synthesized and mixed with *f*CNT to obtain DN hybrid hydrogel with improved modulus and $T_{gelation}$. The effects of H_2O_2 oxidation and *f*CNT addition on the gelling and physico-chemical features of the prepared OGG-*f*CNT hydrogels were investigated. The OGG and prepared OGG-*f*CNT DN hydrogels were characterized by SEM, FTIR, zeta potential, contact angle, and $T_{gelation}$ measurements to evaluate H_2O_2 oxidation and CNT effects on the physicochemical properties. While the degree of $T_{gelation}$ after oxidation is successfully reduced below physiological temperature, this temperature was further lowered by mixing with *f*CNT. The synthesized DN hydrogel showed an increasing modulus from 1389 Pa to 4895 Pa with *f*CNT. The morphological structure of the OGG-*f*CNT DN hydrogel system was significantly affected by the addition of *f*CNT. This study for the OGG-*f*CNT hydrogel system demonstrated the interaction between components and the properties of a three-dimensional GG structure can be affected by oxidation and the presence of *f*CNT. The obtained observations from this study may be necessary for the application of GG as a biomaterial in tissue engineering and drug carrier in delivery systems.

Article info

History:
Received: 02.07.2021
Accepted: 27.10.2021

Keywords:
Double networked hydrogel,
Gellan gum,
Oxidation,
Rheological analysis.

1. Introduction

Hydrogels are a subject that continues to increase rapidly and attracts attention from scientists [1]. The spatial harmony of the liquid form of the gel systems between the implant formed and the randomly shaped places, their drug loading capabilities, and adjustable modulus values put hydrogels among essential research topics in the biomedical field [2]. On the other hand, in cell cultivation studies, the rapid gelation process is at the forefront as it causes a uniform distribution of the transplanted cells into the biomaterial [3]. All these ideal features of hydrogels bring with it more prospects and research to develop new hydrogel materials to meet the ever-increasing requisitions of tissue engineers and biomaterials. Since hydrogels are water-containing 3D structures, they are also used in drug release applications such as wound healing, especially due to their ability to encapsulate water-soluble drug molecules. In addition, it is also used in the field of tissue engineering by adding additions to the hydrogels in accordance with the mechanical strength of the target tissue.

Gellan gum (GG) is an extracellular polysaccharide, water-soluble, anionic and contains α-L-rhamnose (Rhap), β-D-glucose (Glcp), β-D-glucuronic acid (GlcpA), and β-D-glucose (Glcp) repeating units [4]. Due to its biological, physical, and chemical behavior, a suitable heat and acid resistant biomaterial, and its biodegradability, biocompatibility, and low cytotoxicity, GG has been explored its use in nanomedicine, bioengineering, and tissue engineering [5–7]. Physicochemical modification facilitates the applications of GG in different fields. Produced on an industrial scale at low cost, GG is also used in wound dressing preparation to prevent postoperative wound formation and suppress adhesions [8].

Homogeneous distribution of thermally reversible gelling GG can be obtained at 85-90°C [9]. The 3D mesh formation begins with lowering the temperature, with many free random GG coils interacting with the

*Corresponding author. *e-mail address: serbulentturk.@sakarya.edu.tr*

junction areas to form a double helix structure. With the complexation of multiple cations supporting the strengthening of the hydrogel architecture, adjacent carboxyl groups can help the gelation process. However, some disadvantage of physical cross-linking of GG include gelling temperature incompatibility with most cell therapy strategies, in-vivo instabilities over time due to the exchange of cations. Therefore, many studies have been performed examining how to improve its stability and lower the gelation temperature [10].

Since the Tgelation of pure GG is too high (>42°C) for injectable cell carriers, it must be brought to physiological temperature (~37.5°C) so that it can transport cells and be used in minimally invasive injectable applications. In addition, since they have poor mechanical strength, their strength needs to be improved for successful applications as tissue engineering scaffolds and carrier materials [11]. Modifying the structure of GG with the use of cross-linking agents (e.g., (1-ethyl-3-(3-dimethylaminopropyl)carbodiimide) that are toxic to cells causes a long gelation time. In this study, it is assumed that the design of a system that can both add strength and obtain a double network structure and the oxidation of GG can overcome these limitations and improve its functional properties.

Oxidation is an ideal method for adding carboxyl groups, increasing water solubility, and reducing the gelling temperature to physiological values. Due to the poor solubility of pure carbon nanotube (CNT), functionalized CNT (*f*CNT) with oxygen-containing functional groups on its surface is often used as supplementary material for biomedical applications. For instance, because of a great number of active hydroxyl groups on both oxidized GG and *f*CNT chain, the interconnection occurs between them, resulting in the ionic cross-linking of *f*CNT OG form stable hydrogels. This study aims to develop a hydrogel composed of different concentrations of *f*CNT and OGG to promote convenient features for the reasons mentioned above. To achieve this purpose, it has been oxidized the GG with H_2O_2 and then to obtain a DN hydrogel through the −H bond reactions it has been further combined OGG with *f*CNT. Investigations have shown that there is no hydrogel study in the literature examining the properties of OGG-*f*CNT structure oxidation and CNT addition.

2. Materials and Methods

2.1. Materials

Gellan gum (GG, trade name Phytagel), hydrogen peroxide (H_2O_2, 30% in aqueous), copper sulfate ($CuSO_4$), multi-walled carbon nanotube (CNT), and calcium chloride ($CaCl_2$), were purchased from Sigma Aldrich. Throughout the study, purified water obtained by Millipore Milli-Q was used in the synthesis and solution preparation steps.

2.2. Synthesize of oxidized GG

To synthesize the OGGs, 2 g of GG was dissolved in 60 mL of deionized water at 85°C in a sealed bottle to prevent water loss. After cooling to 50°C, 0.05% $CuSO_4$ solution (4 mL) was added, and 30% H_2O_2 was added at different rates (20, 40, and 60 mL) with stirring, then allowed to react at room temperature for 48 h. After the prepared mixture was dialyzed to remove H_2O_2 and Cu^{2+}, the lyophilization step was started. After freezing at −20°C for 12 h, it was lyophilized (BIOBASE) at 15Pa for 2 days at −50°C. After that, the lyophilized hydrogels were stored in sealed bottles. The OGGs were denoted as OGG_1, OGG_2, and OGG_3 when the rates of H_2O_2 were 20, 40, and 60 mL, respectively.

2.3. Preparation of OGG-*f*CNT DN hydrogels

Lyophilized OGG and *f*CNT were dissolved in deionized water at rates of 2.5% (w/v) and 1% (w/v), respectively, under constant mixing for 15 min at 85°C. The *f*CNT was obtained by functionalizing CNT by refluxing it with nitric acid, as in our previous study [12]. To prepare GG-*f*CNT, OGG_1-*f*CNT, OGG_2-*f*CNT, and OGG_3-*f*CNT hydrogels for each sample 15 mg/mL of *f*CNTs mixing with 1% w/v OGG, OGG_1, OGG_2, and OGG_3, respectively. To obtain the well-dispersed *f*CNT in the DN hydrogel, *f*CNT was sonicated by probe sonication (Q Sonica Sonicator) in distilled water for 10 min at an amplitude of 15% in pulsed mode (1.0 seconds pulse on/off) and then transferred into the hot OGG solutions. Afterward, 0.1% (w/v) $CaCl_2$ was added and stirred for 15 minutes to produce cross-linked hydrogels. The prepared solutions were cooled to room temperature to obtain three-dimension OGG-*f*CNT DN hydrogels.

2.4. Characterization of hydrogels

Molecular groups and bindings in pure gellan gum (PGG), oxidized GGs, and prepared OGG-*f*CNT samples were characterized using FTIR (Spectrum Two Perkin-Elmer Co.). The prepared samples were

scanned at 4 cm^{-1} resolution in the 4000 cm^{-1}-400 cm^{-1} wavelength range.

Gelation temperature of PGG and OGGs and OGG-*f*CNT were measured according to the inverting approach. The OGG-*f*CNT hydrogel solutions were added to the centrifuge tubes after dissolving in the distilled water at 85°C. Tubes were then incubated in a temperature-monitored water bath (Nuve, ST 30) to determine the gelation point. The temperature of the water bath, which was initially kept higher than the $T_{gelation}$ to avoid gelation of samples, was gradually lowered. The tubes (n=5) in which the samples were placed before gelation was removed from the water bath for observation after the temperature stabilized every 5 min and the current temperature at which the solutions lost their fluidity was recorded as the $T_{gelation}$.

The morphologies of hydrogels were investigated by scanning electron microscopy (SEM, JEOL, JMS 6060). Lyophilized hydrogels were cut into suitable pieces before observation. After fixation on conductive carbon tapes, they were analyzed after coating them with a thin layer of gold by sputtering (Polaron CS7620) to ensure conductivity. Pore sizes were measured with Image J software using SEM micrographs of lyophilized OGG-*f*CNT hydrogels.

PGG, OGGs, and OGG-*f*CNT were dissolved in distilled water at a concentration of 0.1% (w/v) at 70°C. The zeta potentials of the samples were then measured at 25°C (Nano-Plus).

4 µl of distilled water was dropped on the lyophilized hydrogel with the help of a Hamilton syringe, and contact angles were measured using a goniometer (Attention) with sessile drop method at room temperature. Since the porosity in the surface morphology may affect the contact angle, the measurements of the samples pressed into flat surfaces were carried out to obtain a flat surface by minimizing the effects of the porous morphology of the lyophilized samples. Average contact angle values collected 5 s after drop deposition were obtained using a video-enabled optical system.

The rheological properties of OGG-*f*CNT DN hydrogels were investigated after they were placed in the measuring cell of the rheometer and covered with paraffin oil to avoid the evaporation of the water in it. Sweep tests of angular frequency (ω) with a frequency range between 1 and 100 rad s^{-1} of OGG-*f*CNT DN hydrogels adjusted at 0.5 mm thickness and fixed at 1% strain (γ) were performed at 25°C.

3. Results and Discussion

It has been analyzed that the FTIR spectrums of PGG and OGGs have characteristic peaks around 3367, 2912, 1727, 1609, 1405, and 1029 cm^{-1}, as can be seen from Fig. 1 (a). While the band formed at approximately 2912 cm^{-1} corresponds to the C−H stretching vibrations of sugar, the peaks corresponding to the symmetric and asymmetric stretching vibrations of the carboxyl groups of the salt form were observed at 1405 cm^{-1} and 1609 cm^{-1}, respectively. The band belonging to the C−O−C stretch was observed around 1029 cm^{-1}. A new characteristic peak around 1727 cm^{-1} in the spectra of all OGGs was analyzed, which was followed to become more pronounced in proportion to oxidation. It is known that the peak around 1715 cm^{-1} corresponds to the C=O stress peaks of aldehydes, esters, and carboxylic acids. Peaks belonging to the carboxylic group were observed in the dissociated form at 1727 cm^{-1} and in the salt form at around 609 cm^{-1}-1405 cm^{-1} [13]. Thus, a new characteristic peak increase of about 1727 cm^{-1} appeared for all OGGs, indicating the formation of carboxylic groups in OGGs after oxidation. [14]. The new peak intensity increase, indicating that the amounts of carboxyl groups in the OGGs increased with increasing oxidation degree, demonstrated successful incorporation of carboxyl groups into GG.

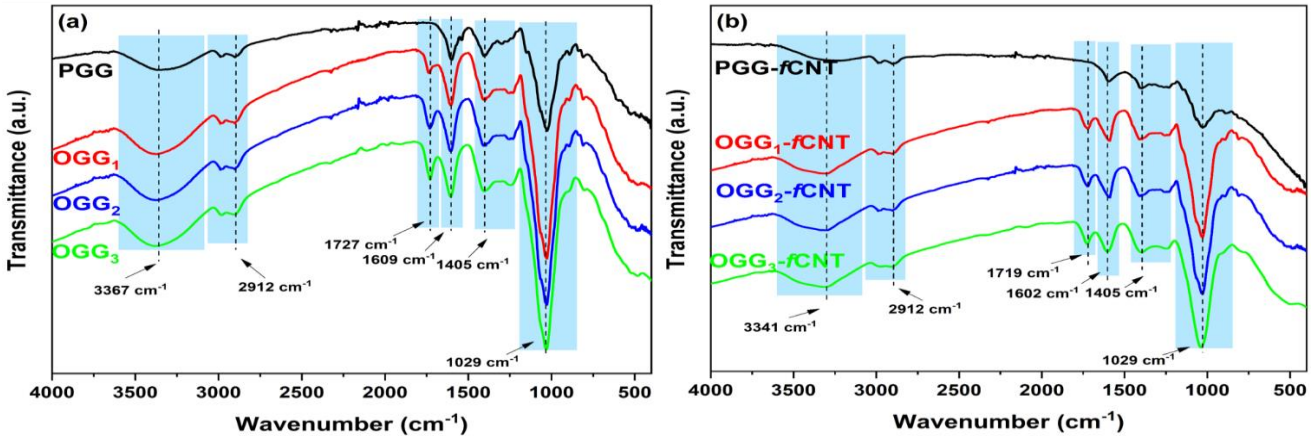

Figure 1. (a) FTIR spectra of PGG, OGG_1, OGG_2, and OGG_3,. (b) FTIR spectra of OGG-*f*CNT DN hydrogels.

Fig. 1b was FTIR spectra of OGGs/*f*CNT hydrogels. No noticeable difference was appeared between the groups, only a slight shift after DN hydro-gelation. The peak at 1719 cm^{-1} indicates that OGG participates in the gelation and takes place in the hydrogels prepared by preserving its original structure.

As can be seen in Fig. 2a, $T_{gelation}$ values of PGG, OGG_1, OGG_2, and OGG_3 samples prepared at 2.5% (w/v) concentration differ. PGG exhibited a high gelling temperature of 43°C, while the gelling temperatures of OGG_1, OGG_2, and OGG_3 were 39°C, 32°C, and 29°C, respectively. After oxidation, the $T_{gelation}$ temperatures of GG significantly reduced with the increase of H_2O_2 amount.

Fig. 2b shows how $T_{gelation}$ values change with the addition of *f*CNT. It was observed that the $T_{gelation}$ temperature of the OGG_3-*f*CNT sample obtained by adding *f*CNT to the OGG_3 sample, which has a high oxidation degree, was the lowest. Decreasing the $T_{gelation}$ temperatures of OGG samples with *f*CNT can be attributed to the inhibition of the electrostatic interaction between the OGG chains. It is thought that the temperature of the gelation phenomenon, which considers the formation of stabilized double helix junction sites, decreases by increasing the interaction in unit volume with the oxidation of hydroxyl groups of GG and addition of *f*CNT.

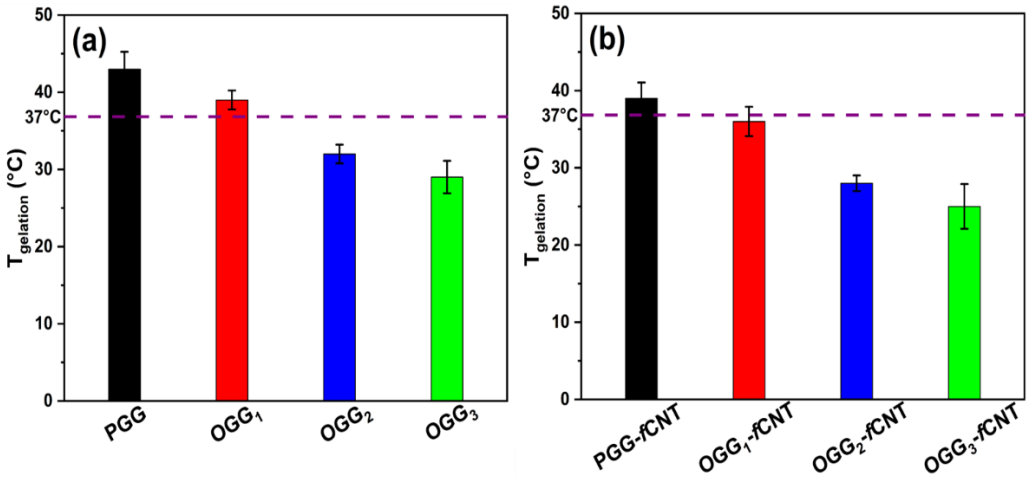

Figure 2. (a) Gelation temperature of PGG, OGG_1, OGG_2, and OGG_3. (b) Gelation temperature of PGG-*f*CNT, OGG_1-*f*CNT, OGG_2-*f*CNT, and OGG_3-*f*CNT. (n= 5).

As presented in Table 1, the charge density of PGG, OGGs, and OGG/*f*CNT DN hydrogels was characterized by measuring their zeta potential values. The zeta potentials of the PGG, GG samples showed a negative value because of the presence of carboxyl groups in the repeating units of the molecules. In addition, after oxidation, OGG_1-OGG_3 samples were characterized as having lower negativities with zeta potentials in the range of −12.4 mV to −28.3 mV. These increased negative zeta potential values were attributed to incorporating more carboxyl groups. In addition, it was observed that the charge densities of OGG-*f*CNT DN hydrogels increased with the addition of CNT. This decrease in zeta potential supports the presence of oxygen-containing functional groups on the *f*CNT surface. With the increase of functional groups containing oxygen in the hybrid hydrogel, it was found as −16.2, −27.1 and −31.4 for OGG_1, OGG_2 and OGG_3, respectively, after *f*CNT addition. Therefore, OGG-*f*CNT products with DN structure can be obtained containing OGG, which has the desired negativity for oxidation and application with *f*CNT.

Table 1. Zeta potential of pristine, oxidized, and *f*CNT added DN structured hydrogels.

Hydrogels	Zeta-potential (mV)
PGG	−8.2±0.3
OGG_1	−12.4±0.2
OGG_2	−22.6±0.8
OGG_3	−28.3±0.9
PGG-*f*CNT	−11.6±0.2
OGG_1-*f*CNT	−16.2±0.5
OGG_2-*f*CNT	−27.1±0.8
OGG_3-*f*CNT	−31.4±1.1

To investigate the effect of *f*CNT addition on morphology, OGG_3 and OGG_3-*f*CNT hydrogels were examined by SEM, as shown in Fig. 3. Prepared cylindrical hydrogels (a1 and b1) were lyophilized and morphologically analyzed after cutting to the appropriate size. It has been observed that the hydrogels prepared with interconnected and homogeneous porosity have different pore sizes. While the pore size of the OGG_3 hydrogel was found to be 523±87 μm, the pore size of the OGG_3-*f*CNT hydrogel after the addition of *f*CNT decreased to 238±43 μm and was observed to be more compact than OGG_3. There was no apparent phase separation in OGG_3-*f*CNT, and the results support that *f*CNT is homogeneously dispersed into the hydrogel network with a porous structure. The structure of OGG_3-*f*CNT with uniform and small pores has been attributed to the increased crosslinking density in its structure.

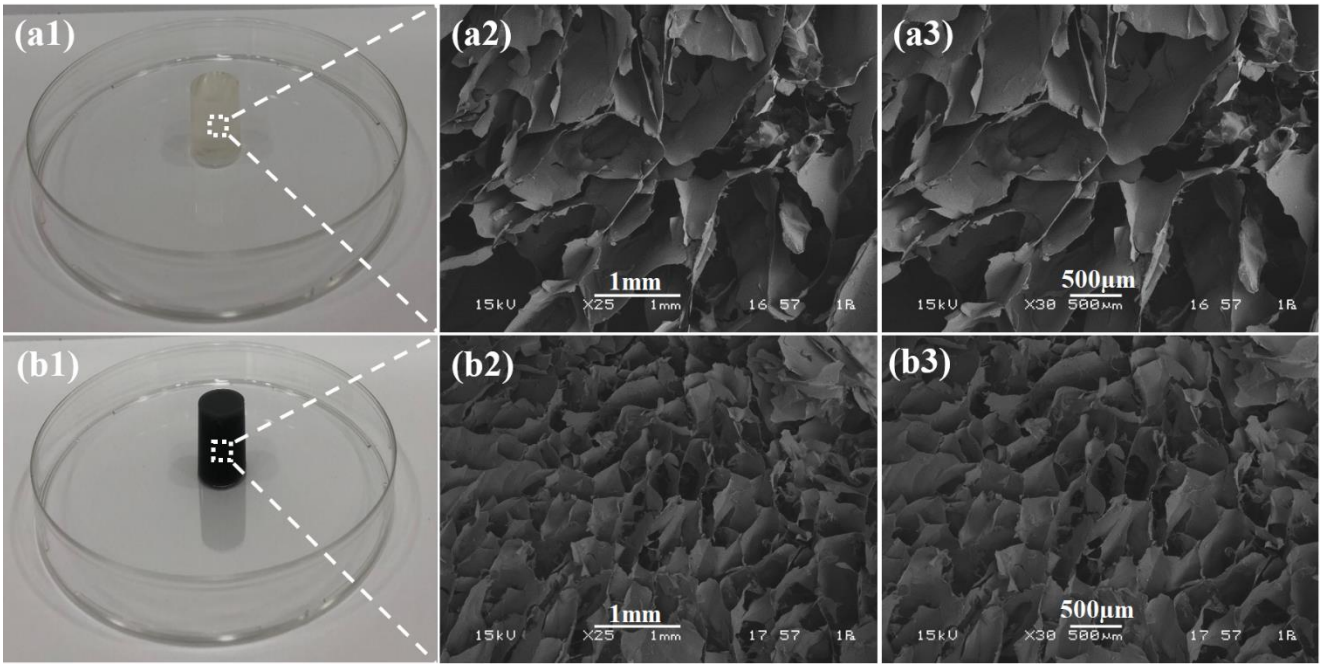

Figure 3. Prepared cylindrical (a1) OGG_3 and (b1) OGG_3-*f*CNT hydrogels, and SEM images of the cross-section of lyophilized (a2, a3) OGG_3 hydrogels and (b2, b3) OGG_3-*f*CNT hydrogels.

The storage (*G'*) and loss modulus (*G''*) of OGG_3 and OGG_3-*f*CNT DN hydrogels at a constant test temperature of 25°C were investigated depending on the frequency as seen in Fig. 4.

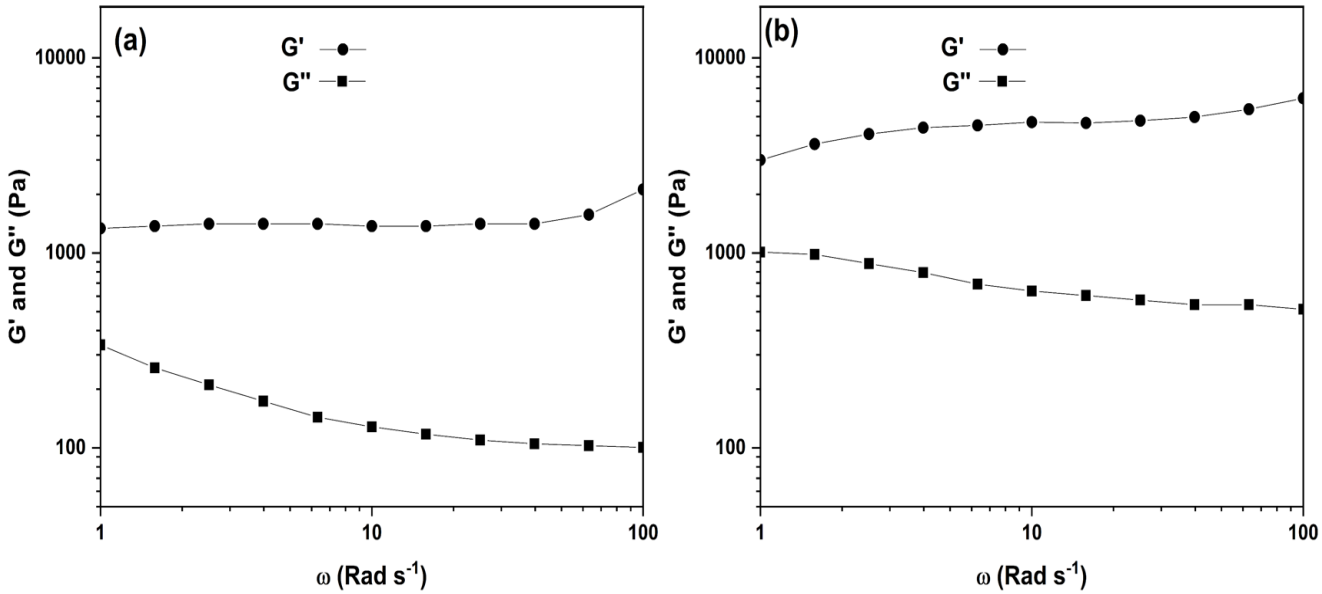

Figure 4. Storage modulus (*G'*) and loss modulus (*G''*) of the prepared (a) OGG_3 and (b) OGG_3-*f*CNT hydrogels.

When the modulus values of both hydrogels are examined, G'' is lower than G' indicates that the hydrogel samples exhibit a solid-like behavior. It was observed that hydrogels with higher modulus values were obtained after the increase of the G' value after the addition of *f*CNT. For example, at a frequency of 40 rad s^{-1}, the mean modulus for OGG without CNT was 1389 Pa, while it increased to an average of 4895 Pa after *f*CNT addition. This result shows that with CNT, the G' and G'' values can be adjusted to the desired values for the OGG/*f*CNT DN hydrogel. The OGG-*f*CNT hydrogel produced for engineering bone tissue requires a strong and relatively hard gel, or, conversely, for applications of tissues such as heart or corneal tissue, which requires a much softer and more elastic gel, can be adjusted. These site-related factors need to be considered when optimizing a hydrogel to culture a specific tissue. Based on this result, the adjustment of the properties of the OGG-*f*CNT hydrogel produced to suit the tissue to be cultured and the in vitro modulus of the hydrogels that reflect the in vivo environment can be performed. As shown in Fig. 5, measurements of contact angle five seconds after drop deposition on all gel types' surfaces were performed to investigate the oxidation and *f*CNT effects further. When the contact angles of the pristine (a1) and oxidized GG samples (a1-a4) were examined, it was observed that the contact angle decreased as a result of oxidation. This decrease is attributed to the increase of oxygen-containing functional groups formed due to oxidation on the surface. In the *f*CNT added hydrogel samples, it was concluded that the wettability of the hydrogel samples was increased by the addition of *f*CNT because of the presence of oxygen-containing functional groups on the surface of *f*CNT. Since the contact angle is related to the interactions between the material and the water molecules, it is generally concluded that the water interacts less with the unoxidized and *f*CNT-free GG hydrogel sample.

Hydrogen peroxide (H_2O_2), which has a pKa of 11.6, is more acidic than water and decomposes into the unstable perhydroxyl anion (HOO^-) with heat. Then, it reacts with H_2O_2 to form a highly reactive hydroxyl radical (HO•). The formation steps of these reactions are shown in Equations 3.1, 3.2, and 3.3 as follows:

$$H_2O_2 \rightarrow H^+ + HOO^- \quad (3.1)$$

$$HOO^- \rightarrow HO^- + (O) \quad (3.2)$$

$$H_2O_2 + HOO^- \rightarrow HO\cdot + H_2O + O_2^- \quad (3.3)$$

Free hydroxyl radicals (HO•) abstract hydrogen atoms from GG's C_6 and form –COOH groups. As mentioned above, hydroxyl groups are formed due to oxidation steps, including the oxidation steps of C6 hydroxyl to carbonyl groups and carboxyl groups. The GG oxidation steps from the presence of H_2O_2 are shown in Scheme1a.

Scheme 1b showed that DN hydrogels were prepared by cross-linking *f*CNT and calcium cross-linked OGG. The oxidation reaction increased the cross-linking allowed for both entangled networks formation. Gelation is mainly because of the H bond reaction between OGG and *f*CNT. In the DN hydrogel system, OG was pretreated with Ca^{2+} for physical crosslinking since known that the presence of the cation is required to form a stable hydrogel via electrostatic interaction. Mixed with $CaCl_2$, linked by H bonds, DN hydrogels were also ionically cross-linked via electrostatic interactions.

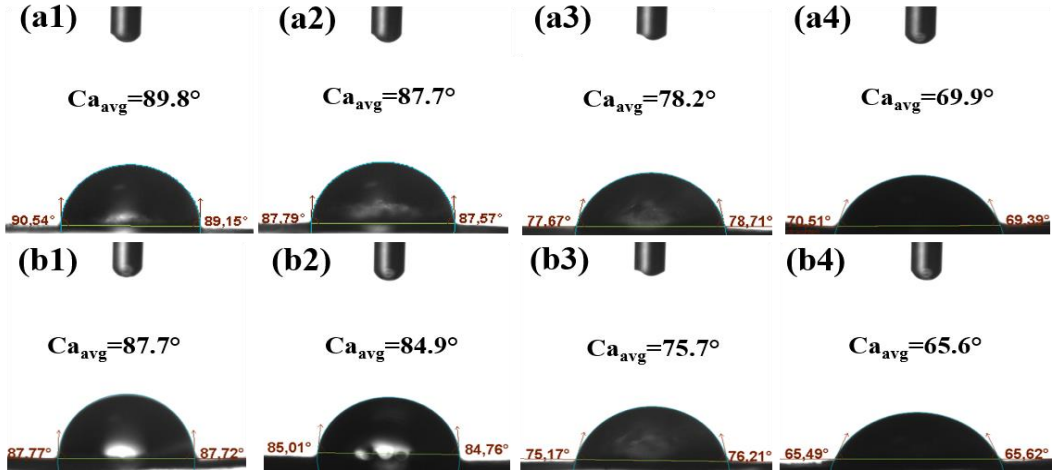

Figure 5. Contact angle measurements of (a1) PGG, (a1) OGG, (a2) OGG_1, (a3) OGG_2, (a4) OGG_3 hydrogel samples before *f*CNT addition and (b1) PGG-*f*CNT, (b2) OGG_1-*f*CNT, (b3) OGG_2-*f*CNT, and (b4) OGG_3-*f*CNT hydrogel samples after *f*CNT addition.

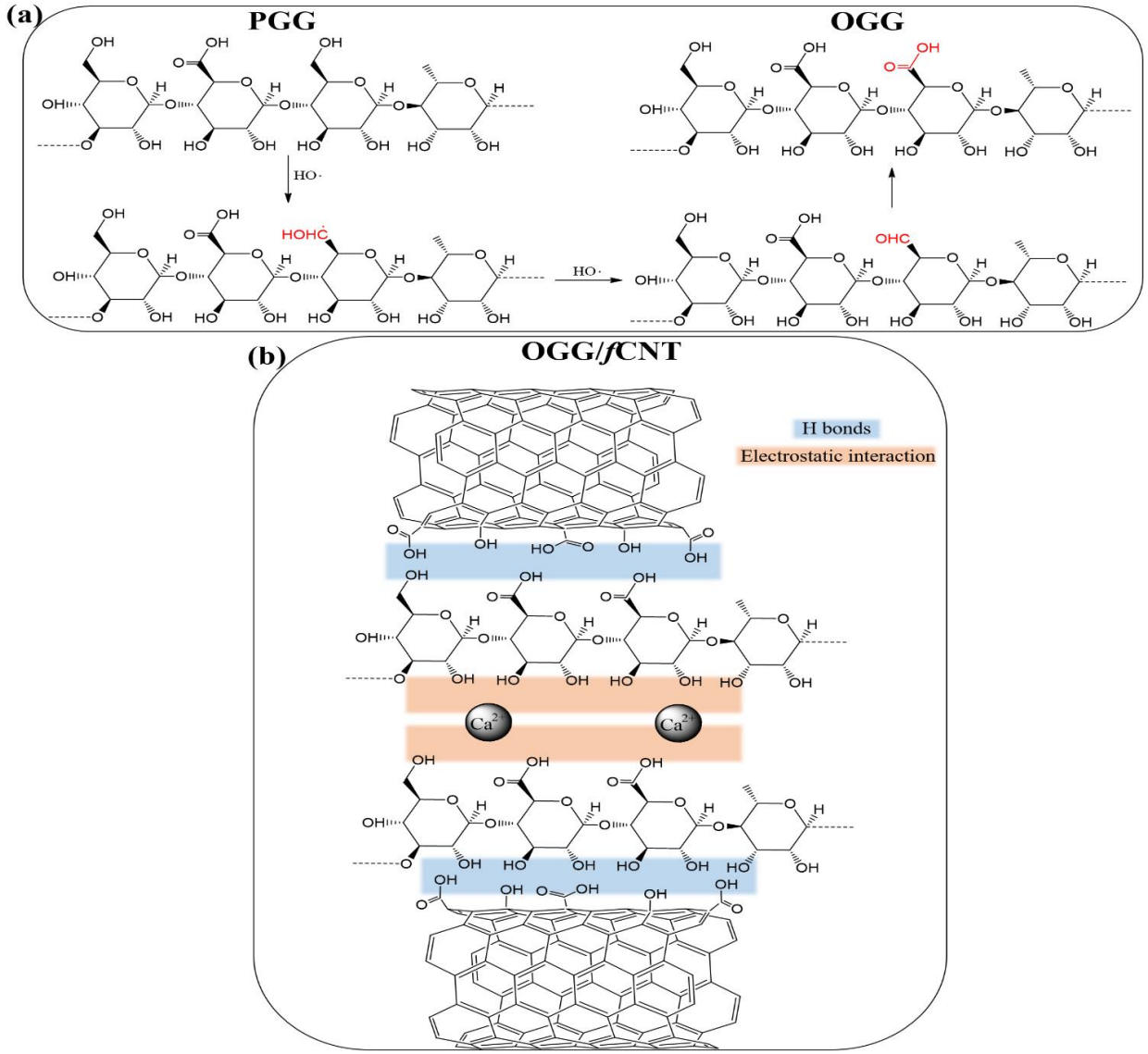

Scheme 1. (a) The overall reaction of GG oxidation in the presence of H_2O_2. (b) Demonstration of structure and interactions in double networked OGG/*f*CNT hydrogels.

In this study, a new hydrogel was successfully developed with oxidation gellan and *f*CNT. The DN structure was formed by the ionic cross-linking method, including both Ca^{2+} cross-linking and hydrogen bonding. The results obtained from the modulus and $T_{gelation}$ were found to be promising for the prepared hydrogel, as it has a wide range of use and adjustable properties. FTIR, Zeta, and contact angle measurements confirmed the successful incorporation of carboxyl groups into GG molecules. The OGG-*f*CNT hydrogel exhibited a higher wettability with increasing oxidation amount.

Moreover, the gelation temperature and zeta potential of OGGs significantly changed depending on *f*CNT addition and degree of oxidation. The added *f*CNT greatly influenced the morphology of fabricated OGG-*f*CNT hydrogel. The OGG_3-*f*CNT hydrogel showed a high modulus compared to 4895 Pa for OGG without *f*CNT and was 1389 Pa. As a result, this study presents innovative hydrogel composed of OGG and *f*CNT that can be used as biomaterials in tissue engineering and as carriers in various drug delivery systems as potential applications.

It is believed that in future studies, GG-based hydrogels obtained with the addition of CNT, which is known to be conductive, will also take part in self-healing strain sensor studies and will be a strong candidate as a new material for use in sensitivity studies against sensitive movements such as pulse, which is one of the requirements of this field.

Acknowledgments

This work was supported by the Scientific Research Projects Commission of Sakarya University (Project number: 2019-6-23-223). The author thanks Dr. Muaz Kemerli for assisting with rheological studies.

Conflicts of interest

The authors state that they did not have any conflict of interests.

References

[1] Mondal S., Das S., Nandi A.K. , A review on recent advances in polymer and peptide hydrogels, *Soft Matter*, 16 (2020) 1404–1454.

[2] Dorishetty P., Dutta N.K., Choudhury N.R., Bioprintable tough hydrogels for tissue engineering applications, *Advances in Colloid and Interface Science*, 281(102163) (2020) 1-23.

[3] Yang J., Zhang Y.S., Yue K., Khademhosseini A. , Cell-laden hydrogels for osteochondral and cartilage tissue engineering, *Bone Research*, 5(17014) (2017) 1–20.

[4] Bonifacio M.A., Cometa S., Cochis A., Gentile P., Ferreira A.M., Azzimonti B., Procino G., Ceci E., Rimondini L., De Giglio E. , Antibacterial effectiveness meets improved mechanical properties: Manuka honey/gellan gum composite hydrogels for cartilage repair, *Carbohydrate Polymers*, 198 (2018) 462–472.

[5] Kouhi M., Varshosaz J., Hashemibeni B., Sarmadi A., Injectable gellan gum / lignocellulose nano fi brils hydrogels enriched with melatonin loaded forsterite nanoparticles for cartilage tissue engineering : Fabrication, characterization and cell culture studies, *Materials Science & Engineering C*, 115(111114) (2020) 1–12.

[6] Palumbo F.S., Federico S., Pitarresi G., Fiorica C., Giammona G. , Gellan gum-based delivery systems of therapeutic agents and cells, *Carbohydrate Polymers*, 229(115430) (2020) 1-19.

[7] Liu S., Qiu Y., Yu W., Zhang H. , Highly Stretchable and Self-Healing Strain Sensor Based on Gellan Gum Hybrid Hydrogel for Human Motion Monitoring, *ACS Applied Polymer Materials*, 2(3) (2020) 1325–1334.

[8] Zhang X., Pan Y., Li S., Xing L., Du S., Yuan G., Li J., Zhou T., Xiong D., Tan H., Ling Z., Chen Y., Hu X., Niu X. , Doubly crosslinked biodegradable hydrogels based on gellan gum and chitosan for drug delivery and wound dressing, *International Journal of Biological Macromolecules*, 164 (2020) 2204–2214.

[9] Osmałek T.Z., Froelich A., Jadach B. , Rheological investigation of high-acyl gellan gum hydrogel and its mixtures with simulated body fluids, *Journal of Biomaterials Applications*, 32(10) (2018) 1435–1449.

[10] Mohammadinejad R., Kumar A., Ranjbar-Mohammadi M., Ashrafizadeh M., Han S.S., Khang G., Roveimiab Z. , Recent Advances in Natural Gum-Based Biomaterials for Tissue Engineering and Regenerative Medicine: A Review, *Polymers*, 12(176) (2020) 1-38.

[11] Wang D., Li C., Gong Y., Wang C., Lai R.C., Su K., Zhang F., Wang D. , An improved injectable polysaccharide hydrogel : modified gellan gum for long-term cartilage regeneration in vitro, *Journal of Materials Chemistry*, 19(14) (2009) 1968–1977.

[12] Türk S., Altınsoy I., Çelebi Efe G., Ipek M., Özacar M., Bindal C. , 3D porous collagen/functionalized multiwalled carbon nanotube/chitosan/hydroxyapatite composite scaffolds for bone tissue engineering, *Materials Science & Engineering C*, 92 (2018) 757–768.

[13] Lu Y., Zhao X., Fang S. , Characterization, Antimicrobial Properties and Coatings Application of Gellan Gum Oxidized with Hydrogen Peroxide, *Foods*, 8(31) (2019) 1–12.

[14] Wang P., Luo Z., Xiao Z. , Preparation, physicochemical characterization and in vitro release behavior of resveratrol-loaded oxidized gellan gum/resistant starch hydrogel beads, *Carbohydrate Polymers*, 260(117794) (2021) 1-10.